# Perturbation evolution with a nonminimally coupled scalar field

Rachel Bean
*Theoretical Physics, The Blackett Laboratory, Imperial College, Prince Consort Road, London SW7 2BZ, United Kingdom*
(Received 3 May 2001; published 27 November 2001)

We recently proposed a simple dilaton-derived quintessence model in which the scalar field was nonminimally coupled to cold dark matter, but not to ''visible'' matter. Such couplings can be attributed to the dilaton in the low energy limit of string theory, beyond the tree level. In this paper we discuss the implications of such a model on structure formation, looking at its impact on matter perturbations and CMB anisotropies. We find that the model only deviates from ΛCDM and minimally coupled theories at late times, and is well fitted to current observational data. The signature left by the coupling, when it breaks degeneracy at late times, presents a valuable opportunity to constrain nonminimal couplings given the wealth of new observational data promised in the near future.

DOI: 10.1103/PhysRevD.64.123516 PACS number(s): 98.80.Cq

## I. INTRODUCTION

There is recent evidence [1–3] that the Universe's expansion is accelerating. If this is so, it would have fundamental cosmological implications, for progressing the dark matter problem and reconciling a high Hubble constant, $h \sim 0.65$, with an old Universe $t_0 > 11$ Gyr. To explain such an acceleration, the Universe would have to have a matter component, additional to ordinary matter and radiation, since the latter two have equations of state that are unable to generate the required kinematics. In line with current observational constraints, the additional matter would have to have an equation of state $p = w\rho$ with $w \in (-1, -0.4)$ [4–6].

A pure cosmological constant cannot explain the observed acceleration without running into fine-tuning problems; one would need $\Lambda \sim 10^{-122} c^3/(\hbar G)$, several hundreds of orders of magnitude lower than one would expect from a vacuum energy originating at the Planck time [7]. This has lead to a wealth of proposals using a scalar ''quintessence'' field, minimally coupled to matter through gravity, which can be cajoled into acting as an effective cosmological constant in the presence of a suitable potential. Models of particular interest use ''tracker'' potentials (e.g. [8–13]) which allow the scalar field to produce the required dynamics without dependence on initial conditions, but these still require small-scale parameters. More recently, a model was proposed [14,15] with a potential whose parameters were, a more physically agreeable, Planck scale. Explaining why the acceleration has only arisen recently, however, still requires some degree of fine-tuning in the model parameters, if not in the initial conditions, in order to confine acceleration to the current epoch [16]. A more practical explanation for the coincidental acceleration nowadays is that we are in close proximity to the cosmological transition from radiation to dust domination. Armendariz-Picon, Mukhanov and Steinhardt [17] utilized this proximity to drive the dynamics of their $\kappa$-essence model although the Lagrangian used is somewhat complex, consisting of a series of nonlinear kinetic terms.

In a recent paper [18], we proposed a simpler model which harnesses the dynamical shift in the radiation-dust transition using a nonminimally coupled (NMC) scalar field. We showed that a coupling of this form can use the transition to dust domination to push a quintessence field off scaling behavior, and produce acceleration in the background nowadays.

In this paper we consider the impact of such a nonminimal coupling on the evolution of perturbations to the background and the subsequent implications for both structure formation and the cosmic microwave background (CMB).

We start by giving an overview of the coupled quintessence model, and then go on to discuss the implications of coupling for perturbation evolution and structure formation.

## II. COUPLED QUINTESSENCE MODEL

Nonminimal theories are commonly expressed in one of two frames. In one, the problem is posed in the Jordan frame and the scalar field is directly coupled to curvature, in the form $f(\phi)\mathcal{R}$, and produces a departure from Einstein's gravity, as is seen in Brans-Dicke theories [19]. This effect was used by [20] to force the quintessence field out of scaling behavior, necessary to give accelerated dynamics, however this ''R-boost'' occurs early in the radiation epoch and cannot explain acceleration today. In the second, the Einstein frame is used and the scalar field instead couples to terms in the matter Lagrangian resulting in dynamical, field-dependent, masses and polarizations. These two groups are interrelated through conformal transformation of the metric; any theory in one frame can be rephrased in the other. However, usually a simple function in one frame is mapped into a complicated function in the other. Such couplings are heavily constrained when applied to the visible matter in the Universe, whether to photons [21], or to what is usually called baryons [22]. However, it could be that the dilaton coupled differently to visible matter and to the dark matter of the Universe. This hypothesis was suggested in [23], and allows for large couplings to be consistent with observations (see also [24,25]). We consider a scenario in which such a case exists.

We choose $g^{\mu\nu}$ to have convention $(+ - - -)$ in a flat Friedmann-Robertson-Walker (FRW) background. All quantities are expressed in units with $M_P = (8\pi G_N)^{-1/2} = 1$ where $M_P$ is the Planck mass and $G_N$ is the Newtonian gravitational constant. We consider a Lagrangian of the form

 

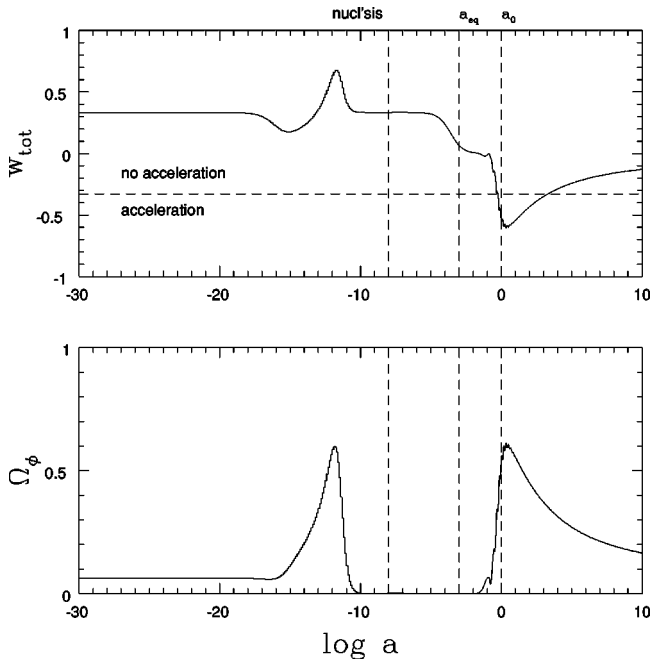


FIG. 1. The evolution of $\Omega_\phi$ and $w_{tot}$ for a model with $\lambda=8$, $\beta=8$, $\alpha=50$, and $\phi_0=32.5$ (and $\Omega_b=0.053, h=0.65$). An early period of scaling is broken near the transition from radiation to matter, first with a period of kination, then inflation. At late times the universe returns to a matter dominated scaling solution.

$$\mathcal{L}=\sqrt{-g}\left(-\frac{R}{2}+\frac{1}{2}\partial_\mu\phi\partial^\mu\phi-V(\phi)+\mathcal{L}_V+f(\phi)\mathcal{L}_c\right) \tag{1}$$

in which $\mathcal{L}_V$ is the Lagrangian of ''visible matter'' (baryons, photons, and also baryonic and neutrino dark matter), and $\mathcal{L}_c$ the Lagrangian of a dominant nonbaryonic form of cold dark matter. We take $V(\phi)=V_0e^{-\lambda\phi}$ the standard quintessence potential, which drives scaling behavior when the coupling is minimal [11,12].

The coupling investigated is of the form $f(\phi)=1+\alpha(\phi-\phi_0)^\beta$. Couplings of this form could arise as generalizations of an effective action for massless modes of a dilaton [22] after performing a conformal transformation from the string frame into the Einstein frame. $\alpha$ and $\beta$ are parameters reflecting the shape of the minimum being approached by the coupling [26].

### A. Background evolution

Here we discuss the background equations in the conformal FRW metric, which are derived in Appendix A. The field equations are obtained by varying the action with respect to the metric and the scalar field:

$$G_{\mu\nu}=T^{(V)}_{\mu\nu}+T^{(\phi)}_{\mu\nu}+f(\phi)T^{(c)}_{\mu\nu} \tag{2}$$

$$\nabla^2\phi=\frac{\partial V}{\partial\phi}-\frac{\partial f}{\partial\phi}\mathcal{L}_c \tag{3}$$

where $G_{\mu\nu}$ is the Einstein tensor and the various $T_{\mu\nu}$ are stress-energy tensors. Heuristically, we may interpret the new term driving $\phi$ as a contribution to an effective potential $V_{eff}=V-f(\phi)\mathcal{L}_c$. Bianchi's identity ($\nabla_\mu G^\mu_\nu=0$) leads to

$$\nabla_\nu T^{\mu\nu(V)}=0 \tag{4}$$

$$\nabla_\nu T^{\mu\nu(c)}=(g^{\mu\nu}\mathcal{L}_c-T^{\mu\nu}_c)\frac{f'}{f}\nabla_\nu\phi. \tag{5}$$

These are to be contrasted with Amendola's coupled quintessence [27] (for which the interaction term is proportional to $T$).

Evaluating the components of the field equations, with scale factor $a$, we find Friedmann equations:

$$\frac{3}{a^2}\left(\frac{\dot a}{a}\right)^2=\rho_b+\rho_\gamma+f(\phi)\rho_c+\frac{1}{2}\frac{\dot\phi^2}{a}+V(\phi) \tag{6}$$

$$\dot\rho_c+3\frac{\dot a}{a}\rho_c=-\frac{f'(\phi)\dot\phi}{f(\phi)}(\rho_c+\mathcal{L}_c)=0 \tag{7}$$

$$\rho_b+3\frac{\dot a}{a}\rho_b=0 \tag{8}$$

$$\rho_\gamma+4\frac{\dot a}{a}\rho_\gamma=0 \tag{9}$$

$$\ddot\phi+2\frac{\dot a}{a}\dot\phi+a^2V'=f'(\phi)\mathcal{L}_c a^2=-f'(\phi)\rho_c a^2 \tag{10}$$

where dots represent derivatives with respect to conformal time, and the prime ($'$) indicates differentiation with respect to $\phi$.

One notices in Eq. (7) that the evolution of the background coupled dark matter is unaffected by the coupling. This simply arises because we are coupling to pressureless matter for which $\mathcal{L}_c=-\rho_c$; if we had instead coupled to radiation we would find $\mathcal{L}=0$ and the coupling would have altered the background evolution (as discussed in Appendix A). However as will be discussed later, observations measure the coupled energy density $f(\phi)\rho_c$ not simply $\rho_c$ so that the magnitude of the observed matter is affected by the coupling through Eq. (10).

Figure 1 shows the evolution of $\Omega_\phi$ and overall equation of state $w_{tot}=\rho_{tot}/p_{tot}$ for one model scenario. One can see that deep in the radiation epoch the coupling has a negligible effect on the overall dynamics and the scalar field's energy density scales with that of the dominant radiation, as in the minimally-coupled case. As the transition from radiation to matter domination is approached the coupling becomes important and the dynamics are driven away from scaling behavior. The driving term on the right-hand side of Eq. (10) first, transiently, drives the field to kinate, suppressing the evolution of the scalar field and $\Omega_\phi\sim 0$, then it re-emerges into inflationary behavior to provide the accelerated expansion we observe today. The model requires that $\beta$ be even

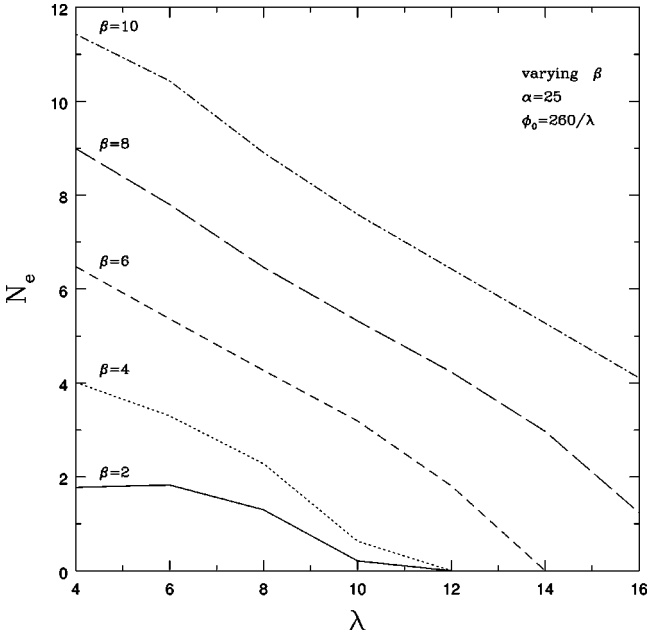


FIG. 2. The amount of accelerated expansion produced with the model for various values of $\beta$, measured in the number of e-foldings $N_e = a_f/a_i$. $a_i$ and $a_f$ are the expansion scales when inflation begins and ends, respectively ($a_i < a_0 \leqslant a_f$, where $a_0 = 1$ is the expansion scale nowadays). We have given $\alpha = 25$ as an example with $\phi_0 = 260/\lambda$.

and that the value of $\phi_0$ is of the order of magnitude of the scalar field today. However given these constraints, the model provides acceleration for a wide range of parameters as shown in the parameter space plots for the nonminimally coupled model in Figs. 2 and 3.

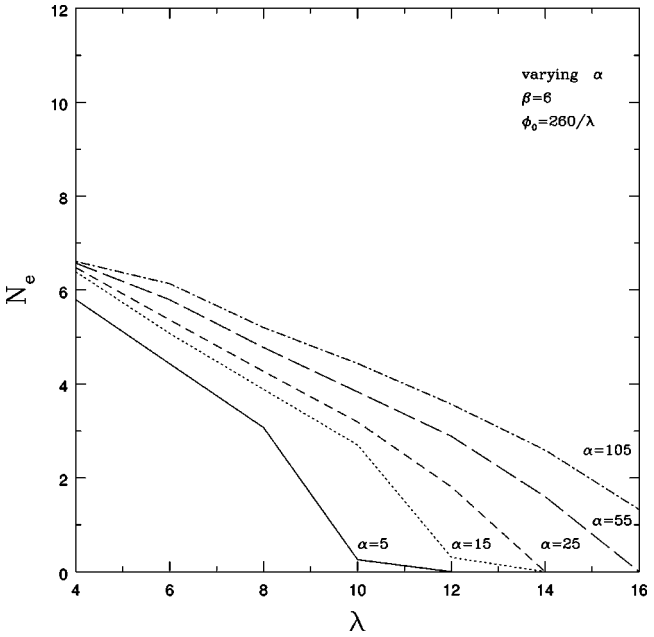


FIG. 3. The amount of accelerated expansion produced with the model as $\alpha$ is varied, measured again in the number of e-foldings $N_e$. We have given $\beta = 6$ as an example with $\phi_0 = 260/\lambda$.

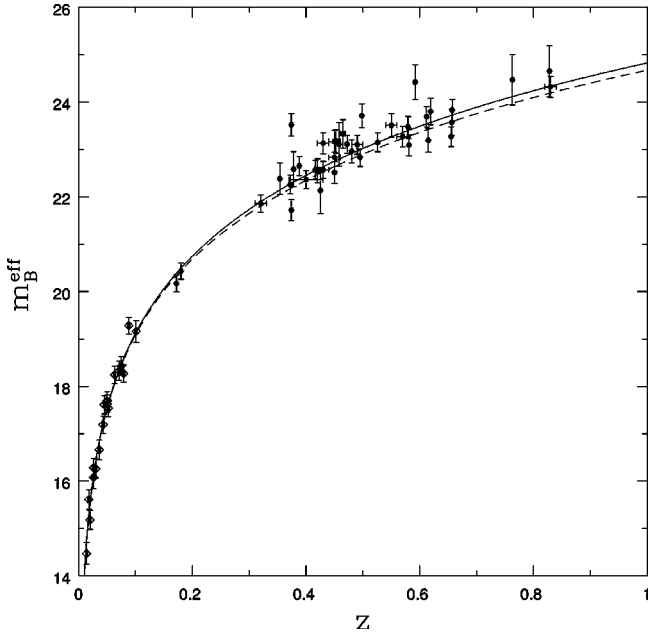


FIG. 4. Plot of the effective bolumetric magnitude for the Calán Tololo (open diamonds) and SCP data points (solid circles) against redshift. The curves correspond to two models considered in this paper; the cold dark matter model with a cosmological constant ($\Lambda$CDM) model (solid line) with $\Omega_c = 0.347$, $\Omega_b = 0.053$ and $\Omega_\Lambda = 0.6$ and a nonminimally coupled model with $f(\phi)\Omega_c = 0.347$, $\Omega_b = 0.053$ and $\Omega_\phi = 0.6$ with model parameters specified in Fig. 1.

In minimally coupled models with exponential potentials, the value of the parameter $\lambda$ is limited by big-bang nucleosynthesis (BBN) constraints [28] to be $\lambda \geqslant 8$; however the NMC model avoids this constraint through the suppression of $\Omega_\phi$ at nucleosynthesis, irrespective of $\lambda$'s value. Parameter constraints for the nonminimal case can only therefore come from CMB and matter power spectrum predictions discussed below. In order to compare the nonminimal models with analogous minimally coupled ones, however, we consider cases with $\lambda = 8$ in our discussion below.

### B. Observational implications

It is pertinent to consider whether the effect of the nonminimal coupling on the background at late times could be seen in current observations, i.e. when looking at the predicted apparent magnitude versus redshift relation at $z < 2$.

The apparent bolumetric magnitude is given by

$$m(z) = M + 5 \log d_L(z) + 25 \tag{11}$$

where $M$ is the absolute bolumetric magnitude, and $d_L$ is the luminosity distance in Mpc

$$d_L = (1+z) \int_0^z \frac{dz'}{H(z')}. \tag{12}$$

In Fig. 4 we plot the effective bolumetric magnitude from the B-band filter, $m_B^{eff}(z)$, from the Calán Tololo [29] and SCP [6] surveys and predicted m(z) curves for the nonminimally

coupled model in Fig. 1 and a comparative ΛCDM model. The effective magnitude is obtained from the apparent magnitude after taking into account the lightcurve width-luminosity correction, galactic extinction and the *K* correction from the differences in the observed *R* band and restframe B-band filters [6]. Within current observational error constraints, the non-minimally coupled model cannot be distinguished from the ΛCDM model. Recently proposed observational projects (see for example [30]) may offer future hope to discriminate between the effect of quintessence models on the background evolution.

In the remainder of the paper, we consider an alternative approach to distinguishing between quintessence models, through their effect not on the background but on the perturbations about it.

## III. IMPLICATIONS FOR STRUCTURE FORMATION

The addition of the scalar field has implications for structure formation both due to the addition to the homogeneous background energy density, and secondly by the generation and evolution of scalar field perturbations. The additional background energy density shifts the equality redshift and alters the angular distance to the last scattering surface. The scalar field also introduces extra terms in the perturbed Einstein equations and opens up the possibility of isocurvature perturbations evolving.

We study the impact of these effects by calculating the linear perturbation equations and specifying the initial conditions. These are then evolved from early on in the radiation epoch when the coupling is unimportant through to nowadays. The matter and CMB power spectra are then calculated and compared with those obtained with minimally coupled models and observations.

### A. Linear perturbation evolution

We follow the approach and notation of Ma and Bertschinger [31] extended by Ferreira and Joyce [12] for minimally coupled scalar fields. A simplified model containing no baryons is used for the discussion, although a full theory containing baryons and relativistic neutrinos is used to obtain the CMB and matter power spectrum predictions presented. The essential results are presented here, while a full derivation of the equations can be found in Appendix B.

Consider perturbations to a flat FRW metric in the synchronous gauge, with line element

$$ds^2 = a(\tau)^2\{-d\tau^2 + (\delta_{ij} + h_{ij})dx^i dx^j\}. \tag{13}$$

We will only be concerned with the scalar modes of the perturbation, for which we can parametrize the metric perturbation as

$$h_{ij} = \int d^3k e^{ik\cdot x}\left[\hat{k}_i\hat{k}_j h(k,\tau) + \left(\hat{k}_i\hat{k}_j - \frac{1}{3}\delta_{ij}6\,\eta(k,\tau)\right)\right] \tag{14}$$

where $h$ is the trace of the metric perturbation. To obtain the linear perturbation evolution equations we consider the perturbed Einstein equations

$$k^2\eta - \frac{1}{2}H\dot{h} = 4\pi G a^2 \delta T^0_0 \tag{15}$$

$$k^2\dot{\eta} = 4\pi G a^2 i k_i \delta T^0_i \tag{16}$$

$$\ddot{h} + 2H\dot{h} - 2k^2\eta = -8\pi G a^2 \delta T^i_i \tag{17}$$

$$\ddot{h} + 6\ddot{\eta} + 2H(\dot{h} + 6\dot{\eta}) - 2k^2\eta = 24\pi G a^2\left(\hat{k}_i\hat{k}_j - \frac{1}{3}\delta_{ij}\right)\Sigma^i_j \tag{18}$$

where $\Sigma^i_j$ is the traceless shear. Writing the perturbations to energy densities, $\rho$, pressures, $p$, and the scalar field, in terms of a homogeneous background plus a perturbation, we have

$$\rho(x,\tau) = \rho(\tau)[1 + \delta(x,\tau)] \tag{19}$$

$$p(x,\tau) = p(\tau) + \delta p(x,\tau) \tag{20}$$

$$\Phi(x,\tau) = \phi(\tau) + \varphi(x,\tau). \tag{21}$$

The only perturbation in $T^\mu_\nu$ to be affected by the coupling is $\delta T^0_0$, the other perturbations are the same as for a minimally coupled model,

$$\delta T^0_0 = -\rho_\gamma\delta_\gamma - (\varphi f' + f\delta_c)\rho_c - \left(\frac{1}{a^2}\dot{\varphi}\dot{\phi} + \varphi V'\right) \tag{22}$$

$$ik_i\delta T^0_i = \frac{4}{3}\rho_\gamma\theta_\gamma + \frac{1}{a^2}\dot{\phi}\nabla^2\varphi \tag{23}$$

$$\delta T^i_i = 3\left(\frac{1}{3}\rho_\gamma\delta_\gamma + \frac{1}{a^2}\dot{\varphi}\dot{\phi} - \varphi V'\right) \tag{24}$$

where $\theta$ is the velocity divergence. The evolution equations of the density perturbations for radiation and the dark matter component are the final requirement. One finds, as is shown in Appendix B, that the coupling does not effect the first order equation for the matter perturbation so that

$$\delta_\gamma = -\frac{4}{3}\theta_\gamma - \frac{2}{3}\dot{h} \tag{25}$$

$$\delta_c = -\theta_c - \frac{1}{2}\dot{h}. \tag{26}$$

The spare degree of freedom in the synchronous gauge allows us to choose the background, synchronous coordinates. As is conventional, we do this by constraining the dark matter field such that $\theta_c = 0$, which fixes $\dot{\delta}_c = -\frac{1}{2}\dot{h}$. We are now able to write down the perturbation equations for the non-minimally coupled system

$$\ddot{\delta}_c + H\dot{\delta}_c + \frac{3H^2\Omega_c f}{2}\delta_c = -3H^2\Omega_\gamma\delta_\gamma - 2\dot{\varphi}\dot{\phi} + \left(a^2V' - \frac{3H^2\Omega_c f'}{2}\right)\varphi \tag{27}$$

$$\ddot{\varphi} + 2H\dot{\varphi} + [k^2 + a^2(V'' + f''\rho_c)]\varphi = -\frac{1}{2}\dot{h}\dot{\phi} - a^2 f'\rho_c\delta_c \tag{28}$$

$$\ddot{\delta}_\gamma - \frac{k^2}{3}\delta_\gamma = \frac{4}{3}\ddot{\delta}_c . \tag{29}$$

The nonminimal coupling introduces extra terms into the equations for matter and scalar field perturbations, altering the mass terms and source terms, the latter shown on the right-hand side of the equality for clarity. The coupling will only affect the radiation perturbations indirectly through the background bulk (via $H$) and through $\ddot{\delta}_c$.

Deep in the radiation epoch, the coupling to dark matter is unimportant. The adiabatic perturbation evolution closely follows the power-law solutions for the minimally coupled model with an exponential potential as discussed by Ferreira and Joyce [12]. The growing modes of $\delta_\gamma, \delta_c$ and $\varphi$ evolve $\propto \tau^2$

$$\delta_\gamma = -\frac{2}{3}C(k\tau)^2, \qquad \delta_c = -\frac{1}{2}h = \frac{3}{4}\delta_\gamma,$$

$$\varphi = -\frac{2}{5\lambda}h, \qquad \dot{\varphi} = -\frac{2}{5\lambda}\dot{h} \tag{30}$$

where $C$ is an arbitrary normalization constant.

It is only at very late times, $z \lesssim \sim 2$, that the coupled matter establishes itself as the dominant effect on growth. This is when we would expect the coupling's signature to start to be seen.

So far only pure curvature (adiabatic) perturbations have been considered, however isocurvature perturbations might also exist in quintessence models [32]. For this nonminimal model we believe that their impact is negligibly small. Isocurvature perturbations are known to be negligible in minimally coupled tracking quintessence models. This will also be so for the nonminimally coupled case early on in the radiation epoch, where the couplings effect is unimportant. When the field is driven off tracking, close to the transition from matter to radiation, we cannot assume this, however. During the period when tracking is broken, the scalar field is suppressed and $\Omega_\phi \sim 0$ (see Fig. 1). In general, the nonadiabatic pressure perturbation $\delta p_{non\text{-}ad}$ is given by

$$\frac{\delta p_{non\text{-}ad}}{\rho + p} = \mathcal{O}(\Omega_\phi)(\delta_\gamma + \delta_\phi). \tag{31}$$

Therefore, since the quintessence contribution to the total energy density is highly suppressed, the isocurvature contributions will continue to be small away from tracking behavior, around the transition time. It is only at very late times, after last scattering, when $\Omega_\phi$ is no longer small, that the isocurvature perturbations may start to grow. For the following discussion, therefore, we only consider adiabatic perturbations.

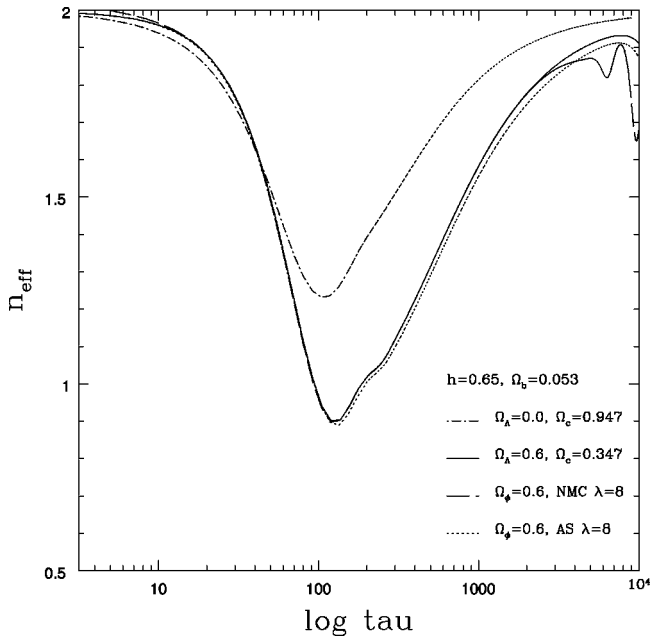


FIG. 5. Time evolution of the effective growth rate for 4 scenarios (all h=0.65, $\Omega_b=0.053$), 3 of which produce acceleration today: (1) ΛCDM $\Omega_\Lambda=0.6$ (full line), (2) NMC model $\Omega_\phi=0.6$, $\lambda=8$, $\beta=8$, $\phi_0=32.5$ (long dash), (3) MC model $\Omega_\phi=0.6$, $\lambda=8$, $A=0.01$, $B=2$, $\phi_0=32.5$ (short dash), and, one which does not, (4) SCDM model $\Omega_c=0.947$ (dot-dash).

### B. Implications for matter perturbations

An important consequence of nonminimal coupling is that, when considering the coupled matter, it is the *coupled energy density*, $f\rho_c$, that should be interpreted as the matter density measured in observations, not $\rho_c$; an analogous case is nonminimally coupled gravity, $f(\phi)\mathcal{R}$, in which we consider the varying gravitational field strength as the observable and not constant Newtonian gravity, $G_N$. So we are interested in the effective dark matter density $\tilde{\delta}_c$

$$\tilde{\delta}_c = \frac{\delta(f\rho_c)}{f\rho_c} = \delta_c + \frac{f'}{f}\varphi. \tag{32}$$

An insightful way to look at the coupling's effect on perturbation growth is by looking at its effect on the dimensionless growth rate

$$n_{eff} = \tau\frac{\dot{\tilde{\delta}}_c}{\tilde{\delta}_c}. \tag{33}$$

In Fig. 5 the growth rate for one scale, $k=0.1$ Mpc$^{-1}$, is shown for various models, in each case h=0.65, $\Omega_b=0.053$. A nonminimally coupled model with $\Omega_\phi=0.6$ and $\lambda=8$ ($\beta=8, \phi_0=32.5$), is compared with a ΛCDM model,

$\Omega_\Lambda = 0.6$, a SCDM model $\Omega_c = 0.947$, and an analogous minimally coupled quintessence model using the potential developed by Albrecht and Skordis [14] $V = V_0 e^{-\lambda\phi}[A + (\phi - \phi_0)^B]$ with $\lambda = 8$ ($A = 0.01$, $B = 2$, $\phi_0 = 32.5$). For $z > 2$ the growth rates for the scalar field models do not differ greatly from that in the $\Lambda$CDM model.

The addition of a scalar field or cosmological constant, with $\Omega_0 = 1$ fixed, will act to reduce $\Omega_c$ and therefore the size of the mass term in Eq. (27). This is the main factor responsible for the suppression of growth at later times, rather than the nonclumping behavior of the scalar field commonly cited as the cause. Subhorizon scalar field perturbations have oscillatory time evolution with decaying amplitudes, their contribution to the evolution of matter perturbations therefore is small for the observationally interesting scales. For NMC models, the coupling suppresses $\Omega_\phi$ around $z_{eq}$, making the scalar field contribution to $\delta_c$ growth negligible. Subsequently, the growth rate for NMC models is closer to that created by a cosmological constant than for the MC models.

At late times however, for $z < 2$, the coupling and scalar field become important, and act to suppress the growth in $\delta_c$ to a far greater extent than $\Lambda$ and MC models, offering a potential way to distinguish nonminimal from minimal the NMC model.

The dampening effect can be also seen in the matter power spectrum P(k),

$$P(k) = \langle |\tilde{\delta}_c(k)|^2 \rangle = (100C) 8\pi^3 h^3 k \left(\frac{k}{k_0}\right)^{n-1} \qquad (34)$$

where $C$ is the normalization factor from CMBFAST [33] arising form the Bunn and White normalization [34] at $l = 10$ multipole, $k$ is in units of $h$/Mpc and $k_0 = 0.05$ Mpc$^{-1}$ and $n$ is the tilt, chosen here $n = 1$ for a scale invariant spectrum.

In Fig. 6 the matter power spectra for the both the NMC and MC models mimic a $\Lambda$CDM model for scales $k < \sim 0.1$ i.e. those modes having entered the horizon before and around equality. There is a slight suppression but a bias factor could in theory resolve the discrepancy. Certainly all three models give reasonable predictions for matter fluctuations over a sphere of size $8h^{-1}$ Mpc with $\sigma_8 = 0.89, 0.91, 1.13$ for NMC, MC and $\Lambda$CDM models, respectively, in comparison to the observed value $\sigma_8 = 0.56\Omega_m^{-0.47} \sim 0.9$ [35].

For larger scales, however, the coupling does make a difference. In scales that have only entered the horizon in recent times, whilst the coupling is important, we see a distinctive reduction of power in comparison to the MC and $\Lambda$CDM models which tend to similar behavior. Although the suppression clearly distinguishes the coupled model, its profile is still consistent with current observational results [36]. There may be an opportunity with the future SLOAN galaxy survey results to constrain the power spectrum at these larger scales (to $k \sim 0.01$).

Another potential impact of the late time importance of the coupling is that it will affect small scale features at $z \sim 2$, observable potentially through future weak lensing (see e.g. [37] and references therein) and damped Lyman $\alpha$ cloud measurements (see e.g. [38]).

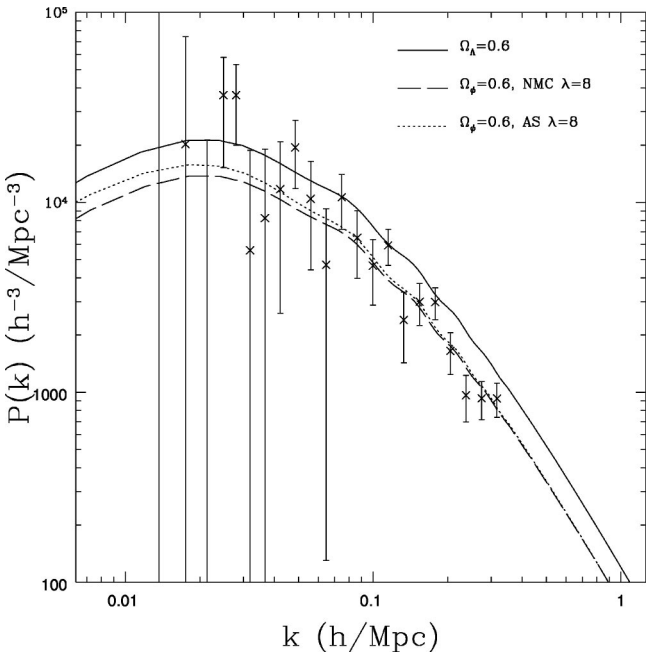


FIG. 6. Matter power spectrum for the 3 scenarios in Fig. 5 which produce acceleration today: $\Lambda$CDM (full), NMC (long dash) and MC (short dash), together with the de-correlated data points of Hamilton *et al.* Parameters in the 3 models are the same as in Fig. 5.

### C. Impact on CMB anisotropies

Introducing a scalar field can potentially have several effects on the CMB power spectrum. Firstly, as we have already mentioned in Sec. III A, the scalar field gives rise to extra mass and source terms in the linear evolution equations for $\varphi$ and $\delta_c$. These then indirectly affect the radiation perturbations, altering the acoustic peak positions and heights at the time of last scattering ($\tau_{lss}$). However, the scalar perturbations are effectively negligible around $z_{eq}$, especially in the NMC scenario, so this effect will be minimal.

Secondly, the time varying Newtonian potential after decoupling will be affected by the coupling, altering the anisotropies produced at large angular scales (the integrated Sachs-Wolfe effect). This can be seen in Fig. 7 where the NMC model has a different profile at small $l$ from the MC and $\Lambda$CDM models. However the effect is not large enough to be disentangled from the effect of cosmic variance.

Thirdly, the inclusion of the scalar field alters the composition of the energy density, altering the angular diameter distance of the acoustic horizon size at recombination. This can be parametrized by the value of $\mathcal{B}$

$$\mathcal{B} = \Omega_c^{1/2} h \int_{z_{rec}}^{z_0} dz \{\Sigma \Omega_j z^{3(1+w_j)}\}^{-1/2}. \qquad (35)$$

Altering the value of $\mathcal{B}$ shifts the positions of the peaks. The critical problem one confronts when trying to use CMB spec-

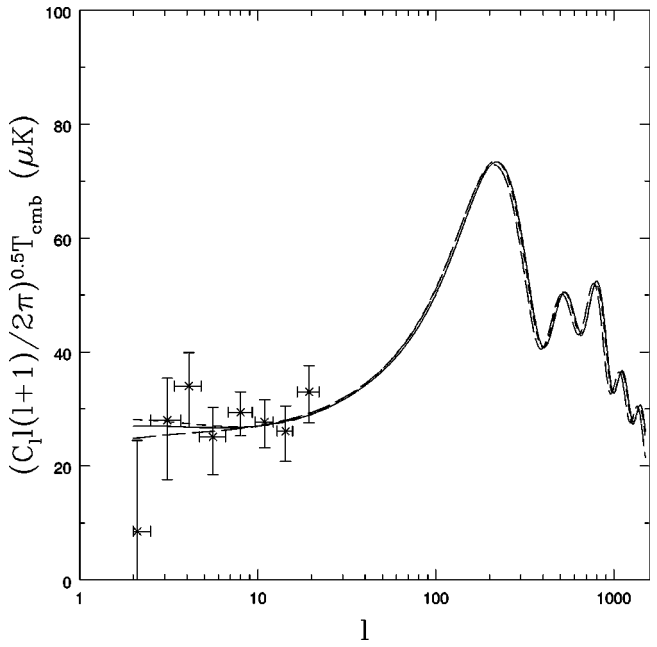


FIG. 7. CMB power spectra showing low $l$ (plateau) behavior for the 3 scenarios in Fig. 5: ΛCDM (full), NMC (long dash) and MC (short dash) with COBE datapoints. Model parameters are the same as in Fig. 5. The 3 models evolve differently at late times producing slightly different ISW anisotropies shown in the plateau at low $l$. However, observations at this scale are dominated by cosmic variance, so that the differences would not be observable.

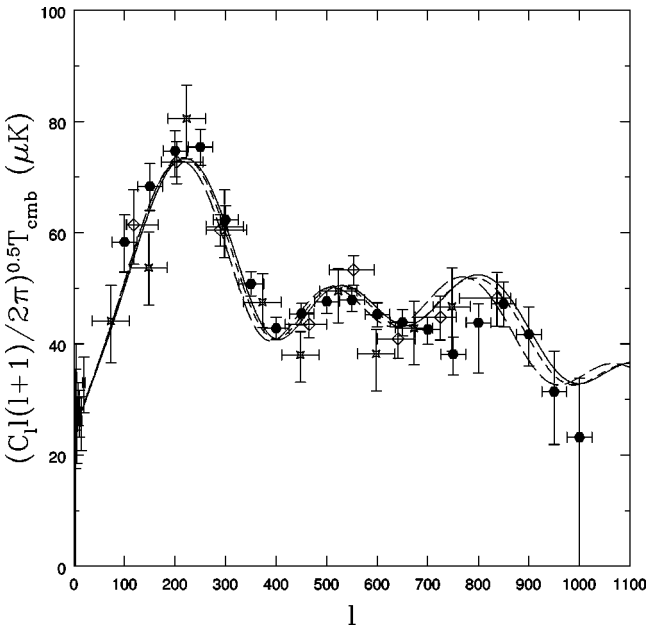


FIG. 8. CMB power spectra showing acoustic peaks for the 3 scenarios in Fig. 5: ΛCDM (full), NMC (dash) and MC (short dash), together with the data from Boomerang (solid circles), Maxima (crosses) and DASI (open diamonds). Model parameters are the same as in Fig. 5.

tra to differentiate between models is the degeneracy that exists between models with identical $\Omega_c$, $\Omega_b$ and $\mathcal{B}$ [39]. It has been shown that this degeneracy can be broken for scalar field models in which a large fraction of the energy density at $\tau_{lss}$ is from the scalar [28]; the scalar field acting as an effective increase in the number of relativistic degrees of freedom. However for models in which $\lambda \geqslant 8$ the degeneracy still exists in minimally coupled models. In Figs. 7 and 8, CMB spectra are plotted for the scenarios discussed in the previous section against Cosmic Background Explorer (COBE) [40], MAXIMA [41], Boomerang [42] and DASI [43] data. All the models discussed have $\mathcal{B}=1.77$ and yet one can see that the degeneracy of the first peak is slightly broken, with the NMC model having $l_{peak}=215$ in comparison to 224 for both the MC and ΛCDM models. It is also interesting to note that the CMB spectra for coupled models with different λ values are effectively degenerate in themselves, as shown in the figure. This implies that, although coupling itself may be distinctive, CMB spectra will not be able to isolate the parameter in the potential.

The fourth possible effect is on the separation of the peaks. This has been proposed as a possible mechanism with which to distinguish minimally coupled models [44]. They are not distinguishable from ΛCDM if $\Omega_\phi(\tau_{lss})$ is small however, as mentioned above. But in the case of non-minimally coupled models the degeneracy in the second and third peaks *is* broken because of the effect the coupling has on $\tau_0$ the conformal time nowadays. This is of particular interest given the expected improvements in peak definition (e.g. [42,41,43,45]). The separation of the peaks $dl$ is given by

$$\delta l = \pi \frac{\tau_0 - \tau_{lss}}{r_s} \tag{36}$$

where $r_s$ is the sound horizon and $c_s$, the baryon speed of sound, both of which can be assumed effectively constant across the models. The NMC model has $\tau_0 = 12\,530$ in comparison to $\tau_0 = 13\,077$ for the ΛCDM model. This reduces the separation slightly breaking the degeneracy, as shown; the separation of the first and second peaks in the NMC model is $dl = 309$ in comparison to 327 ΛCDM scenario.

Although distinguishable from the cosmological constant spectrum, the difference is still too small to be resolved with current observational data, including the most recent Boomerang [42] and DASI [43] data, showing highly improved definition in the second and third peaks. However with a number of observational projects continuing to focus attention on resolving the higher peaks, the breaking of degeneracy may offer a way to constrain non-minimally coupled models. In Fig. 9 we plot the residual differences between the ΛCDM and NMC $C_l$ spectra in Fig. 8 when compared with estimated Microwave Anisotropy Probe (MAP) errors. The parameters used to estimate the MAP errors are shown in Appendix C. The estimated errors are considerably smaller than these residual levels for $l<900$ implying that we may be able to distinguish between these various models within the near future.

## IV. CONCLUSION

We have examined the impact a scalar field, non-minimally coupled to cold dark matter will have on the evolution of matter and radiation perturbations. We considered

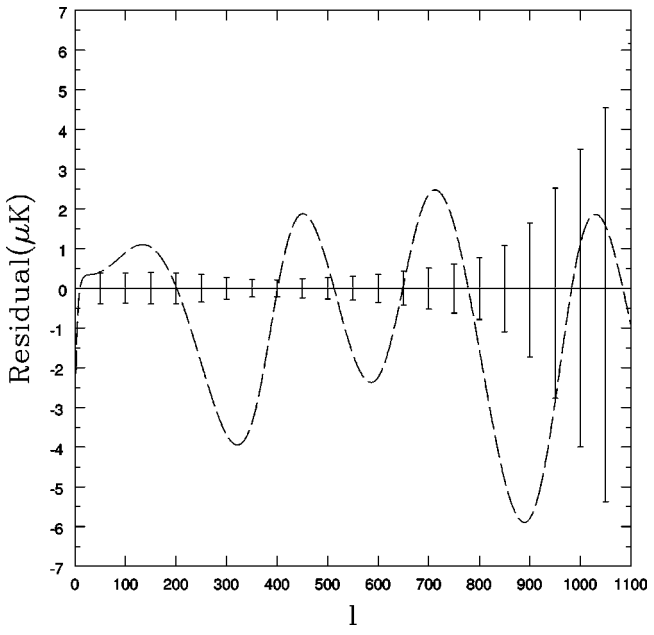


FIG. 9. Residual deviation of the NMC model's temperature fluctuations from those of the ΛCDM model, both shown in Fig. 8, with estimated MAP error bars.

first its impact on the linear evolution equations and found that even though it did introduce new terms these were effectively negligible for all but very late times. The impact of this late time behavior was then considered for matter perturbations where it was seen to create a suppression of growth at large scales. The coupling was also found to break the degeneracy usually seen in the CMB spectrum, slightly shifting the position of the first peak and reducing the separation between adjacent peaks. These two distinctive ''signatures'' of the coupled dark energy model are not resolvable with current observations. However projects currently underway look to mapping both the matter power spectrum and CMB peaks with much improved accuracy. These may offer an opportunity to eventually distinguish between ΛCDM, minimally coupled and nonminimally coupled quintessence models in the near future.

## ACKNOWLEDGMENTS

I would like to thank João Magueijo and Carlo Contaldi for many helpful conversations throughout this work. R.B. acknowledges financial support from PPARC.

## APPENDIX A: BIANCHI'S IDENTITY

In this section we derive the equations of motion for the coupled dark matter and scalar fields explicitly from the action

$$\mathcal{S}=\int \sqrt{-g}d^4x\left(-\frac{\mathcal{R}}{2}+\frac{1}{2}\phi_{,\mu}\phi^{,\mu}-V(\phi)+\mathcal{L}_V+f(\phi)\mathcal{L}_c\right). \tag{A1}$$

Bianchi's identity reflects the symmetry of the Riemann tensor, the Einstein tensor being convariantly conserved,

$$\left(\mathcal{R}^{\mu\nu}-\frac{1}{2}g^{\mu\nu}\mathcal{R}\right)_{;\nu}=[T^{\mu\nu(\phi)}+T^{\mu\nu(V)}+f(\phi)T^{\mu\nu(c)}]_{;\nu}=0. \tag{A2}$$

Since visible matter is minimally coupled in the model we can immediately separate it out,

$$T^{\mu\nu(V)}_{;\nu}=0. \tag{A3}$$

Using the explicit definition of the energy momentum tensor in terms of their Lagrangian,

$$T^{\mu\nu}_{;\nu}=\left[\frac{2}{\sqrt{-g}}\left(\frac{\partial(\sqrt{-g}\mathcal{L})}{\partial g_{\mu\nu}}\right)\right]_{;\nu} \tag{A4}$$

so the scalar field component of the Bianchi identity in terms of $\phi$ and its derivatives is

$$T^{\mu\nu(\phi)}_{;\nu}=\phi^{,\mu}(\phi^{,\nu}_{;\nu}+\Gamma^{\nu}_{\alpha\nu}\phi^{,\alpha}+V'(\phi)). \tag{A5}$$

The Euler-Langrange equation, which is just the Klein Gordon equation, allows us to simplify this further

$$\phi^{,\alpha}_{,\alpha}+\Gamma^{\beta}_{\alpha\beta}\phi^{,\alpha}+V'(\phi)=f'(\phi)\mathcal{L}_c. \tag{A6}$$

Combining these two expressions we obtain

$$T^{\mu\nu(\phi)}_{;\nu}=f'(\phi)\mathcal{L}_c g^{\mu\nu}\phi_{,\nu}. \tag{A7}$$

For the coupled matter then,

$$(f(\phi)T^{\mu\nu(c)})_{;\nu}=f'\phi_{;\nu}T^{\mu\nu(c)}+fT^{\mu\nu(c)}_{;\nu}. \tag{A8}$$

Combining the results in Eqs. (A3) and (A7), Bianchi's identity in Eq. (A2) is given by

$$T^{\mu\nu(c)}_{;\nu}=\frac{f'}{f}\phi_{;\nu}(\mathcal{L}_c g^{\mu\nu}-T^{\mu\nu(c)}). \tag{A9}$$

We can obtain an expression for the Lagrangian for perfect fluid by considering it to be a gas of particles with masses $m_a$ and paths $x^i_a$ [46]

$$\mathcal{L}_a(x)=-m_a\delta(x-x_a(t))(-g_{\mu\nu}\dot{x}^{\mu}\dot{x}^{\nu})^{1/2}. \tag{A10}$$

By noting that the length of the 4-velocity $[-g_{\mu\nu}(dx^{\mu}/d\lambda)(dx^{\nu}/d\lambda)]^{1/2}=ds/d\lambda$ equals 1 for dust, this expression simplifies greatly. Averaging over particles in the gas rest frame we find $\mathcal{L}_c=-n\langle m/u^0\rangle$ where $n$ is the particle number density and $u^{\mu}=dx^{\mu}/d\lambda$ is the 4-velocity. For pressureless particles $u^{\mu}=\{1,0,0,0\}$; therefore $\mathcal{L}_c=-\rho_c$.

We can also obtain an expression for the stress-energy tensor from the Lagrangian in an analogous way. Using the relationship between $T^{\mu\nu}$ and $\mathcal{L}$ in Eq. (A4) the stress-energy for a particle is given by

TABLE I. MAP CMB experimental specifications.

| $\nu$ (GhZ) | $\theta_{n,\mathrm{FWHM}}$ | $10^6\sigma$ | $N_{ch}$ |
|---|---|---|---|
| 40 | 28′ | 8.2 | 4 |
| 60 | 21′ | 11.0 | 4 |
| 90 | 13′ | 18.3 | 8 |

$$T_a^{\mu\nu}=m_a\frac{\delta(x-x_a(t))}{\sqrt{-g}}\dot{x}^\mu\dot{x}^\nu u^0. \tag{A11}$$

On averaging over the particles the energy density is $\rho=\langle T^{00}\rangle=n\langle mu^0\rangle$ and the pressure in the $x$-direction is given by $p=\langle T^{11}\rangle=n\langle mu^0(v^1)^2\rangle$ where $v^i=dx^i/dt=u^i/u^0$, for dust therefore $p_c=0$. In addition, in the rest frame there is zero streaming velocity so that $\langle T^{0i}\rangle=n\langle mu^0v^i\rangle=0$.

In this paper we assume that the coupled matter is comprised of cold pressureless dust particles. Putting the expression for $\mathcal{L}_c$ into Eq. (A9), the background evolution equation for non-minimally coupled matter is identical to that in the minimally coupled case:

$$T^{\mu\nu(c)}_{;\nu}=\dot{\rho}_c+3H\rho_c=0. \tag{A12}$$

## APPENDIX B: LINEAR PERTURBATION EQUATIONS

We here derive the linear perturbation equations for the coupled cdm and scalar fields in detail. We assume the notation of Ma and Bertschinger [31] and results of Ferreira and Joyce [12]. Consider perturbations to a flat FRW metric in the synchronous gauge, with line element

$$ds^2=a(\tau)^2\{-d\tau^2+(\delta_{ij}+h_{ij})dx^idx^j\}.$$

By considering the perturbed Euler-Lagrange equation for the scalar field we can obtain the linear evolution equation for $\varphi$:

$$\varphi^{,\alpha}_{,\alpha}+\delta\Gamma^\beta_{\alpha\beta}\phi^{,\alpha}+\Gamma^\beta_{\alpha\beta}\varphi^{,\alpha}+V''\varphi=f''\varphi\mathcal{L}_c+f'\delta\mathcal{L}_c. \tag{B1}$$

Perturbing the particle Lagrangian in Eq. (A10)

$$\delta\mathcal{L}_a=-\delta m_a\delta(x-x_a(t))(-g_{\mu\nu}\dot{x}^\mu\dot{x}^\nu)^{1/2} \tag{B2}$$

and averaging over all dust particles, we have $\delta\mathcal{L}=-n\langle\delta m/u^0\rangle=-\delta\rho_c$. The nonminimally coupled scalar perturbation equation becomes

$$\frac{\ddot{\varphi}}{a^2}+\frac{1}{2}\dot{h}\dot{\phi}+2\frac{\dot{a}}{a}\dot{\varphi}+V''\varphi-\varphi^{,i}_{,i}=-\rho_c(f''\varphi+f'\delta_c). \tag{B3}$$

The perturbed Einstein equations can be used to obtain an expression for $\dot{\delta}\rho$

$$(\rho+P)\theta+3H(\delta\rho+\delta P)+\frac{1}{2}(\rho+P)\dot{h}+\dot{\delta}\rho=0. \tag{B4}$$

We are interested in the interacting dark matter and scalar field, which are not separable in Eq. (B4)

$$f\rho_c\theta_c+3H\delta(f\rho_c)+\frac{1}{2}(f\rho_c)\dot{h}+\frac{d}{d\tau}(\delta(f\rho_c))+\dot{\phi}\frac{\nabla^2\varphi}{a^2}+3H\left(\frac{2\dot{\phi}\dot{\varphi}}{a^2}\right)+\frac{1}{2}\frac{\dot{\phi}^2}{a^2}a^2\dot{h}+\left(\frac{\ddot{\phi}\dot{\varphi}}{a^2}+\frac{\dot{\phi}\ddot{\varphi}}{a^2}+2\frac{\dot{a}}{a}\frac{\dot{\phi}\dot{\varphi}}{a^2}V'\dot{\varphi}+V''\varphi\dot{\phi}\right)=0. \tag{B5}$$

Using the equations of motion for the background and perturbed scalar field we find that Eq. (B5) simplifies substantially. Interestingly, we find that the coupling does not affect the first order dark matter perturbation equation

$$\dot{\delta}_c=-\theta_c-\frac{1}{2}\dot{h}. \tag{B6}$$

With the residual degree of freedom in the synchronous gauge we are free to fix one additional parameter; by convention we set $\theta_c=0$ so that $\dot{\delta}_c=\frac{1}{2}\dot{h}$. Ignoring baryons, for simplicity, the second order perturbation equation becomes

$$\ddot{\delta}_c+H\dot{\delta}_c+\frac{3H^2f\Omega_c}{2}\delta_c=-3H^2\Omega_\gamma\delta_\gamma-2\dot{\phi}\dot{\varphi}+\left(a^2V'-\frac{3H^2\Omega_cf'}{2}\right)\varphi. \tag{B7}$$

## APPENDIX C: MAP ERROR BAR ESTIMATION

The standard error on the estimate of $C_l$, $\Delta C_l$ for an experiment with $N$ frequency channels (denoted subscript $n$), each respectively with angular resolution $\theta_{n,\mathrm{FWHM}}(\mathrm{arcmin})=\theta_n(\mathrm{rad})/60\times\pi/180$ and sensitivity $\sigma_n$ per resolution element, scanning a fraction $f_{sky}$ of the sky in bins of $l$ size $\Delta l$ is given by [47]

$$\Delta C_l\approx\left(\frac{2}{(2l+1)f_{sky}\Delta l}\right)^{0.5}[C_l+\bar{\omega}^{-1}\bar{\mathcal{B}}_l^{-2}]$$

$$\bar{\omega}\equiv\sum_n\omega_n,\qquad\bar{\mathcal{B}}_l^2\equiv\bar{\omega}^{-1}\sum_n\mathcal{B}_{nl}^2\omega_n,$$

$$\omega_n\equiv(\sigma_n\theta_n)^{-2},\qquad\mathcal{B}_{nl}^2\approx e^{-l(l+1)/l_s^2} \tag{C1}$$

where we have assumed that the experimental beam is approximately Gaussian filtering scale $l_s\equiv\sqrt{8\ln 2}\theta_n^{-1}$. We have assumed a useful sky fraction $f_{sky}=0.65$ and $\Delta l=50$, Table I shows the remaining parameters used, taken from [48].

The combined errors in Fig. 9 are therefore $\Delta[C_l(\Lambda\mathrm{CDM})-C_l(\mathrm{NMC})]=\Delta C_l(\Lambda\mathrm{CDM})+\Delta C_l(\mathrm{NMC})$.

[1] S. Perlmutter *et al.*, Astrophys. J. **483**, 565 (1997); The Supernova Cosmology Project, S. Perlmutter *et al.*, Nature (London) **391**, 51 (1998).
[2] B.P. Schmidt, Astrophys. J. **507**, 46 (1998).
[3] A.G. Riess *et al.*, Astrophys. J. **116**, 1009 (1998).
[4] M. Turner and M. White, Phys. Rev. D **56**, 4439 (1997).
[5] L. Wang *et al.*, Astrophys. J. **530**, 17 (2000).
[6] S. Perlmutter *et al.*, Astrophys. J. **517**, 565 (1999).
[7] J.D. Barrow and F.J. Tipler, *The Anthropic Cosmological Principle* (Oxford University Press, London, 1986), p. 668.
[8] C. Wetterich, Nucl. Phys. **B302**, 668 (1988).
[9] B. Ratra and J. Peebles, Phys. Rev. D **37**, 3406 (1988).
[10] J. Frieman, C. Hill, A. Stebbins, and I. Waga, Phys. Rev. Lett. **75**, 2077 (1995).
[11] P. Ferreira and M. Joyce, Phys. Rev. Lett. **79**, 4740 (1997).
[12] P. Ferreira and M. Joyce, Phys. Rev. D **58**, 023503 (1998).
[13] I. Zlatev, L. Wang, and P. Steinhardt, Phys. Rev. Lett. **82**, 896 (1999).
[14] A. Albrecht and C. Skordis, Phys. Rev. Lett. **84**, 2076 (2000).
[15] C. Skordis and A. Albrecht, astro-ph/0012195.
[16] J. Barrow, R. Bean, and J. Magueijo, Mon. Not. R. Astron. Soc. **316**, L41 (2000).
[17] C. Armendariz-Picon, V. Mukhanov, and Paul J. Steinhardt, Phys. Rev. Lett. **85**, 4438 (2000); Phys. Rev. D **63**, 103510 (2001).
[18] R. Bean and J. Magueijo, astro-ph/0007199.
[19] C. Brans and R. Dicke, Phys. Rev. **124**, 925 (1961).
[20] F. Perrotta, C. Baccigalupi, and S. Matarrese, Phys. Rev. D **61**, 023507 (2000).
[21] S. Carroll, Phys. Rev. Lett. **81**, 3067 (1998).
[22] T. Damour and A.M. Polyakov, Nucl. Phys. **B423**, 532 (1994); Gen. Relativ. Gravit. **26**, 1171 (1994).
[23] T. Damour, G. Gibbons, and C. Gundlach, Phys. Rev. Lett. **64**, 123 (1990).
[24] L. Amendola, Phys. Rev. D **60**, 043501 (1999).
[25] J.P. Uzan, Phys. Rev. D **59**, 123510 (1999).
[26] A.A. Tseytlin and C. Vafa, Nucl. Phys. **B372**, 443 (1992); A.A. Tseytlin, Class. Quantum Grav. **9**, 979 (1992).
[27] L. Amendola, Mon. Not. R. Astron. Soc. **312**, 521 (2000); Phys. Rev. D **62**, 043511 (2000).
[28] R. Bean, S. Hansen, and A. Melchiorri, astro-ph/0104162.
[29] M. Hamuy *et al.*, Astron. J. **106**, 2392 (1993).
[30] J. Weller and A. Albrecht, astro-ph/0106079.
[31] C. Ma and E. Bertschinger, Astrophys. J. **455**, 7 (1995).
[32] L.R. Abramo and F. Finelli, Phys. Rev. D **64**, 083513 (2001).
[33] U. Seljak and M. Zaldarriaga, Astrophys. J. **469**, 437 (1996).
[34] E.F. Bunn and M. White, Astrophys. J. **480**, 6 (1997).
[35] P. Viana and A.R. Liddle, Mon. Not. R. Astron. Soc. **303**, 535 (1999).
[36] A.J.S. Hamilton and M. Tegmark, astro-ph/0008392.
[37] H. Hoeskstra, astro-ph/0102368.
[38] C. Ma and E. Bertschinger, Astrophys. J. Lett. **484**, L1 (1997).
[39] G. Efstathiou and J.R. Bond, astro-ph/9807103.
[40] G. Smoot *et al.*, Astrophys. J. Lett. **386**, L1 (1992); C. Bennett *et al.*, *ibid.* **464**, L1 (1996).
[41] S. Hanany *et al.*, Astrophys. J. Lett. **545**, L5 (2000).
[42] C.B. Netterfield *et al.*, astro-ph/0104460.
[43] C. Pryke *et al.*, astro-ph/0104490.
[44] M. Doran *et al.*, astro-ph/0012139.
[45] B.S. Mason *et al.*, astro-ph/0101171.
[46] P.J.E. Peebles, *Principles of Physical Cosmology*, Princeton Series in Physics (Princeton University Press, Princeton, NJ, 1993).
[47] J.R. Bond, G. Efstathiou, and M. Tegmark, Mon. Not. R. Astron. Soc. **291**, L33 (1997).
[48] M. Tegmark *et al.*, Astrophys. J. **530**, 133 (2000).